



Robust and Coordinated Tuning of PSS and FACTS-PODs of Interconnected Systems Considering Signal Transmission Delay Using Ant Lion Optimizer

Raimundo Nonato Diniz Costa Filho¹  · V. Leonardo Paucar¹

Received: 12 January 2018 / Revised: 29 May 2018 / Accepted: 8 August 2018 / Published online: 13 August 2018
© Brazilian Society for Automatics--SBA 2018

Abstract

This paper presents an ant lion optimizer (ALO) that is used to solve the robust and coordinated tuning of power system stabilizers (PSS) and the power oscillation damping (POD) controller of flexible AC transmission system (FACTS) devices in the presence of remote signals in multimachine power systems. The remote signals are used for the damping of interarea oscillation modes and are modeled by Padé approximation. The static var compensator and thyristor-controlled series capacitor, two FACTS most deployed in practical applications, were considered in this study. The ALO algorithm mimics the hunting mechanism of ant lions in nature: where four steps of hunting prey such as entrapment of ants in traps, random walk of ants, elitism and catching preys/re-building traps are implemented. The two test systems which have been used for the application of the proposed methodology for tuning of PSS and FACTS-PODs are the New England–New York 16-generator 68-bus system, and the Brazilian equivalent system modeled with 24 synchronous machines and 107 buses. Results from these simulations demonstrate the applicability of the proposal in which the efficiency of ALO is highlighted as compared to other algorithms used for design of PSS and FACTS-PODs such as particle swarm optimization and sequential quadratic programming.

Keywords Power system stabilizers · Ant lion optimizer · Small-signal stability · Power oscillation damping · Remote signal

1 Introduction

Low-frequency electromechanical oscillations may seriously affect the angular stability and the transmission lines capability of large interconnected power systems (Kundur 1994). Interconnection of power systems pursues important benefits including higher reliability and security, economy in the power generation costs, flexible operation and stability improvement. However, other problems may arise due to interconnection such as necessity of an adequate interarea control (automatic generation control), tuning of controllers of synchronous generators, operation and control of flexible AC transmission system (FACTS) devices, interchange scheduling.

The use of damping sources is required to guarantee the power system dynamic security against low-frequency oscillations. Power system stabilizers (PSS) are the most used controllers in the electricity industry for damping these oscillations. The main function of PSS is to provide damping torque through an additional stabilizing signal to the automatic voltage regulator (AVR) of the generator.

The basic structure of a conventional PSS includes a gain, a washout filter, two blocks of phase compensation and an output limiter (Kundur 1994). The gain and phase-compensation blocks are used to compensate the system phase in the frequency interval of interest. The washout block is used to attenuate the stabilizing signal for low frequencies. If the PSS parameters are adequately tuned, the power system will benefit from a large damping torque and will be able to support a bigger number of disturbances for several operation conditions (Kundur 1994; Rogers 2000).

Despite the fact that power system stabilizers are able to damp local mode oscillations, their contribution for damping interarea modes of interconnected power systems is not entirely satisfactory (Deng et al. 2015). One solution for this problem is the deployment of FACTS devices (Simões

✉ Raimundo Nonato Diniz Costa Filho
raimundo.diniz@ieee.org

V. Leonardo Paucar
lpaucar@ieee.org

¹ Department of Electrical Engineering, Federal University of Maranhão, São Luís, MA, Brazil

et al. 2009) which give more flexibility for system operation. FACTS most used in actual electrical power systems is the static var compensator (SVC) and the thyristor-controlled series compensator (TCSC). Inserting well-tuned (in a robust way with several operating conditions) power oscillation damping (POD) controllers to the FACTS may guarantee the necessary damping for local and interarea oscillation modes. The interarea modes are strongly influenced by the interaction between the mechanical parts of the generators and the electrical part of the power system and also by the interactions between controllers, for example, PSSs and FACTS-PODs, PSSs and governors. However, the damping of power system oscillations is affected by setting the parameters of PSSs and FACTS-PODs, and consequently, a coordinated design among these stabilizers should be considered when a combination of devices is involved (Hassan et al. 2014).

The structure of a FACTS-POD is similar to the conventional PSS, but differs in its operation and its input signal (Menezes et al. 2016; Cai and Erlich 2005). A fundamental issue concerning the design of an effective and robust POD is the selection of an appropriate input signal. A local signal can be used to avoid the use of an auxiliary communication system (Gamino and Araujo 2017), but remote signals (or global signals) contain information about overall network dynamics as opposed to a local signal, which lack adequate observability of some of the significant interarea modes (Chaudhuri and Pal 2004). However, the use of remote signals creates new challenges, such as a time delay caused from the transmission of said remote signal. Time delays of remote signals are one of the key factors influencing the stability of the whole system and damping performance as well. Therefore, considering the delay of time is a necessary requirement during the controller design process (Shakarami and Davoudkhani 2016; Yao et al. 2011).

An efficient damping of both local and interarea oscillation modes may be obtained through the coordinated and simultaneous tuning of PSSs and FACTS-PODs, thus avoiding possible adverse interactions among the parameters of these controllers (Cai and Erlich 2005). Several techniques, both deterministic and stochastic, have been proposed for tuning PSSs and FACTS-PODs in order to maximize the system damping. For example, sequential quadratic programming (SQP) is proposed in (Cai and Erlich 2005; Ke et al. 2011) for tuning PSSs and TCSC; linear programming is used for tuning PSSs and SVC in (Pourbeik and Gibbard 1998); non-linear programming is used for coordinated tuning of PSSs, SVC and TCSC in (Lei and Povh 2001); sequential conic programming for tuning several TCSC, thyristor-controlled phase shifter (TCPS) and SVC (Simfukwe et al. 2012). However, the need for a good initial guess represents a major disadvantage to these techniques (Werner et al. 2003). Artificial intelligence (AI) techniques have also been applied more recently for tuning PSSs and FACTS-PODs, such as: bacte-

ria swarm optimization (Ali and Abd-Elazim 2012), seeker optimization (Afzalan and Joorabian 2013), particle swarm optimization (PSO) (Shayeghi et al. 2010; Menezes et al. 2016), artificial immune algorithm (Khaleghi et al. 2011), genetic algorithms (GA) (Hassan et al. 2014; Fortes et al. 2016), the artificial bee colony (ABC) algorithm (Martins et al. 2017) and the basic variable neighborhood search (VSA) algorithm (Gamino and Araujo 2017; Fortes et al. 2018). But, these works do not consider the use of remote signals.

Recently, a new AI technique called the ant lion optimizer (ALO) has been developed, which was inspired by the phenomenon of antlions hunting ants in nature. ALO is a population-based algorithm similar to GA and PSO, but the number of parameters to be tuned is less than GA and PSO. ALO has been confirmed to be better in solving various mathematical optimization functions compared to some well-known metaheuristics (Mirjalili 2015). The results, presented in (Mirjalili 2015), show that the ALO algorithm is able to solve real problems with unknown search spaces as well. Therefore, a main contribution of this article is the implementation and analysis of the ALO algorithm in the coordinated and simultaneous tuning of the parameters of PSSs and PODs controllers in multimachine power systems, which feature signal transmission delay.

2 Problem Formulation

The small-signal angular stability problem of a multimachine electric power system may be formulated as a set of linear differential equations. It follows the power system model, the structure of controllers, mathematical model of time delay and the optimization problem formulation for coordinated tuning of PSSs and FACTS-PODs.

2.1 Power System Model

The dynamics of the power system submitted to small disturbances is modeled by the linearization of the nonlinear differential equations of the system, representing the state variables by Δx and the algebraic variables by Δr , as shown in matrix form by Eq. (1) and in expanded form by Eq. (2).

$$\begin{bmatrix} \Delta \dot{x} \\ 0 \end{bmatrix} = \begin{bmatrix} J_1 & J_2 \\ J_3 & J_4 \end{bmatrix} \begin{bmatrix} \Delta x \\ \Delta r \end{bmatrix} \quad (1)$$

$$\Delta \dot{x} = \left(J_1 - J_2 J_4^{-1} J_3 \right) \Delta x = A \Delta x \quad (2)$$

Dimension of the state matrix A is $N \times N$, in which N is the number of state variables. The power system angular small-signal stability is assessed using the first stability criterion of Lyapunov through the analysis of eigenvalues of

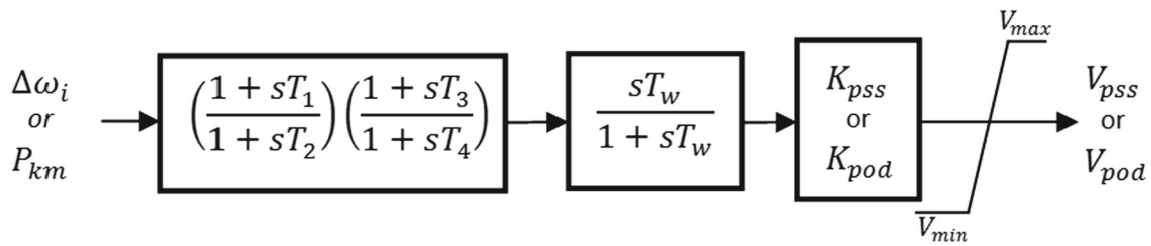


Fig. 1 Structure of PSS and POD

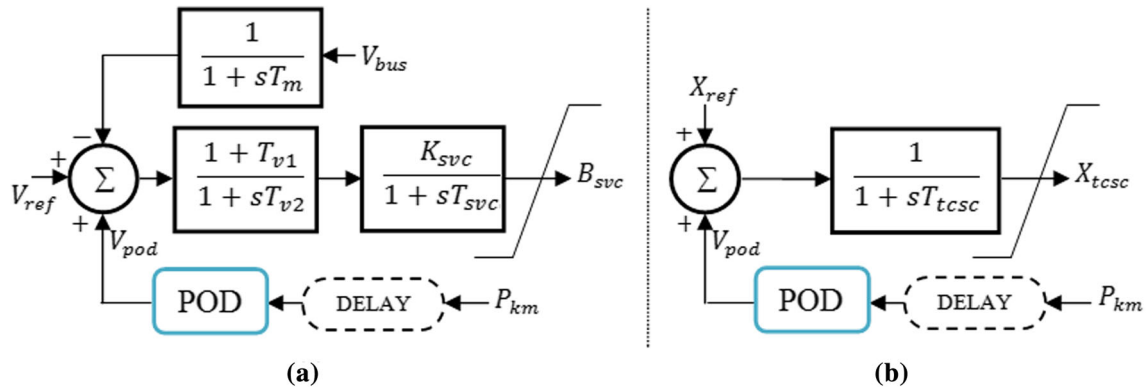


Fig. 2 FACTS block diagram: SVC (a) and TCSC (b)

the state matrix. Modes of electromechanical oscillations are characterized by conjugate complex eigenvalue in the form: $\lambda_i = \sigma_i \pm j\omega_i$. The real part σ_i is related to the exponential growth of response, while the imaginary part ω_i represents the frequency of the respective i th oscillation mode (Kundur 1994).

2.2 Modeling of PSS and FACTS-POD

Several structures for power system stabilizers have been proposed in (Kamwa et al. 2005). In this study, the conventional PSS composed of four blocks is used. This model is shown in Fig. 1 where V_{PSS} is the output signal of PSS, K_{PSS} is the gain of stabilizer, T_w is the time constant of the washout block, T_1-T_4 are the time constants of two phase-compensation blocks, and $\Delta\omega_i$ is the angular speed deviation of the corresponding synchronous machine i .

The installation locations of FACTS devices generally are defined during planning studies of a power system for some objectives such as voltage control, increase power transmission capability, damping of low-frequency oscillations.

In this work the damping of interarea oscillations will be performed mainly through two FACTS: the SVC and TCSC, both equipped with PODs and considering remote transmission signal delay. The input signals to the FACTS devices may be selected by residues. Damping of local oscillations is solved with conventional stabilizers.

The dynamic linearized models of SVC and TCSC are represented in Fig. 2a and b, respectively. In this simplified model of SVC the time constant T_{SVC} is the response time of the thyristor control circuitry, T_m is the time constant involved with the voltage measurement hardware, and T_{v1} and T_{v2} are the time constants of the voltage regulator block (Chaudhuri et al. 2004). Time constant T_{TCSC} of the dynamic model of TCSC corresponds to the firing circuit delay (Deng et al. 2015). The POD controller used in this research has a similar structure to a conventional PSS (Fig. 1). Input signal of POD may, for example, be active power, reactive power, current magnitude, voltage magnitude or angular deviation of synchronous generators. In this study, the active power flow P_{km} of branch $k-m$ has been adopted as an input signal of POD due to its proven efficiency for damping low-frequency electromechanical oscillations (Yang et al. 1998).

2.3 Mathematical Model of Time Delay

The Padé approximation method can be used to study the effect of time delay. The Padé approximation is based on the following property of the Laplace transforms shown in Eq. (3) (Milano 2016):

$$\mathcal{L}\{f(t - \tau)u(t - \tau)\} = e^{-s\tau} F(s) \tag{3}$$

where s is the variable of the Laplace transform \mathcal{L} , $u(t)$ is the unit step function, $F(s)$ is the Laplace transform of the function $f(t)$, and τ is time delay.

Padé approximants are based on the Taylor's expansion of $e^{-s\tau}$. The Padé approximants are expressed as Eq. (4).

$$e^{-s\tau} \approx \frac{1 - K_1s + K_2s^2 + \dots \pm K_ns^n}{1 + K_1s + K_2s^2 + \dots \pm K_ns^n} \quad (4)$$

where n is the order of approximation and K_1, K_2, \dots, K_n are constant coefficients (Shakarami and Davoudkhani 2016).

In this work the first-order Padé approximation is used with coefficients $K_1 = \tau/2$ and $K_2, \dots, K_n = 0$.

2.4 Objective Function

The coordinated tuning of PSSs and FACTS-PODs is formulated as an optimization problem based on the damping ratio ζ_i (see Eq. 5), and the nonlinear objective function is the minimum of F as defined in Eq. (6), subject to a set of constraints of parameters of PSSs and FACTS-PODs given by (7). The objective is to shift all eigenvalues of state matrix into a left-side region limited by a pre-defined damping ratio.

$$\zeta_i = \frac{-\sigma_i}{\sqrt{\sigma_i^2 + \omega_i^2}} \quad (5)$$

where $i=1, 2, \dots, N$, in which N is the total of state variables.

The coordinated tuning of power system stabilizers and power oscillation damping controllers consists of minimizing F in order to obtain the optimal or near-optimal set of PSSs and PODs parameters $\{K_{PSSj} T_{1j} T_{2j} T_{3j} T_{4j} K_{PODk} T_{1k}; T_{2k} T_{3k} T_{4k}, j=1, 2, \dots, N_{PSS}; k=1, 2, \dots, N_{POD}\}$. Constraints are given by (7).

$$\min F = (100 - \zeta_{\min})^2 \quad (6)$$

Subject to,

$$\begin{aligned} \text{lb}_i &= [K^{\min} T_1^{\min} T_2^{\min} T_3^{\min} T_4^{\min}] \\ \text{ub}_i &= [K^{\max} T_1^{\max} T_2^{\max} T_3^{\max} T_4^{\max}] \\ \text{lb}_i &\leq x_i \leq \text{ub}_i \\ \zeta_0 &\leq \zeta_{\min} \end{aligned} \quad (7)$$

where $\zeta_{\min} = \min_{1 \leq y \leq n_y} (\min_{1 \leq q \leq N} \zeta_q)$, ζ_q is the damping ratio of the q th eigenvalue, n_y is the number of operating conditions, ζ_0 (positive value) is a constant value of the expected damping ratio defined by the user for PSSs and PODs design, x_i is a decision variable, and ub_i and lb_i are the upper and lower bounds on the parameters of the PSSs and PODs.

For solving the robust and coordinated tuning of PSSs and PODs of interconnected systems the ant lion optimizer

has been selected because it is a recent metaheuristics with potential to solve efficiently complex and large-scale engineering problems. Some merits of ALO algorithm are, for example, an enhanced exploration of the solution space, local optima avoidance, exploitation and quick convergence, reduced number of variables.

3 The Ant Lion Optimizer

This section will describe the ant lion as a predator and the algorithm emulating the way it traps its prey.

3.1 The Ant Lion Insect

The ant lion (also ant-lion or antlion) is a group of species of insects in the family *Myrmeleontidae* and is most applied to the larval form, often called the doodlebug. Adult ant lions are winged insects that resemble dragonflies. The ant lion larvae construct small cones or funnel-shaped pits in fine, dry soil to trap its prey which are, primarily, ants. The average size of a trap is 5 cm deep and 7.5 cm wide at the edge. To avoid crater avalanches, ant lions construct pits with optimal slope considering the critical angle of repose of the sand (Fertin and Casas 2007; Guillette et al. 2009).

After the pit is complete, the ant lion patiently awaits its prey to fall into the bottom of its trap. When an inattentive ant or other small arthropod steps inside the rim of the trap, it falls to the bottom and will be captured by the ant lion. If the prey attempts to climb up the walls of the pit, it is brought down by a storm of loose sand grains which are thrown at it from the bottom of the trap by the ant lion (Guillette et al. 2009).

3.2 Basics of Ant Lion Optimizer

A strategy for simplifying nonlinear optimization problems based on the ant lion method was proposed earlier in (Stillinger and Weber 1988). More recently, the bio-inspired artificial intelligence technique, ant lion optimizer or ALO, was developed by Mirjalili (2015) to solve optimization problems based on the predatory behavior of ant lion larva.

The mathematical model of ALO is able to reproduce the interaction between the ant lions and the ants, their favorite prey (Fertin and Casas 2007). The bidimensional positions of ant lions and ants are stored in matrices which are started randomly. At any iteration the position of every ant related to the position the ant lion is obtained and updated using roulette-wheel selection and elitism. If the fitness of an ant is better than the respective ant lion, it means that the ant lion captured its prey and assumes this position. At any iteration the best fitness of ant lions is compared to the previous one and is updated if there was an improvement. The ant lion

optimizer makes an adequate exploration and exploitation of search space, which, consequently, is able to approximate the global optimum of optimization problems.

3.3 Antlion: Features

There are four steps to hunting prey: the entrapment of ants in traps, the random walk of ants, elitism and catching preys/re-building traps (Mirjalili 2015; Chen et al. 2017).

3.3.1 The Entrapment of Ants in Traps

For mathematically modeling the behavior of entrapment of ants in traps, the following Eqs. (8) and (9) are proposed:

$$c^t = \frac{c^t}{I}, \quad d^t = \frac{d^t}{I} \tag{8}$$

In Eq. (8), $I = 10^{\frac{w}{T}t}$, t is current iteration, T is the maximum number of iterations, and w is a constant that depends on current iteration whose values are given by Eq. (9).

$$w = \begin{cases} 2 & \text{if } t > 0.1T \\ 3 & \text{if } t > 0.5T \\ 4 & \text{if } t > 0.75T \\ 5 & \text{if } t > 0.9T \\ 6 & \text{if } t > 0.95T \end{cases} \tag{9}$$

3.3.2 Random Walks of Ants

Ants generally walk randomly in nature when searching for food; hence, their walk is supposed to be stochastic in behavior. This behavior is expressed mathematically by the following equations (Chen et al. 2017):

$$X(t) = [0, c_s(2r(t_1) - 1), \dots, c_s(2r(t_{\max}) - 1)] \tag{10}$$

where c_s denotes cumulative sum, t_{\max} is the maximum number of iterations, t shows the iterations of random walk, and $r(t)$ is a stochastic function defined by (11).

$$r(t) = \begin{cases} 1, & \text{if } \text{rand} > 0.5 \\ 0, & \text{if } \text{rand} \leq 0.5 \end{cases} \tag{11}$$

Here rand represents a uniformly distributed random number between 0 and 1.

In order to keep the random walks inside the search space, they are normalized using (12).

$$X_i^{t+1} = \frac{(X_i^t - a_i)(d_i^t - c_i^t)}{b_i - a_i} + c_i^t \tag{12}$$

In Eq. (12), a_i and b_i are the minimum and maximum of random walks of the i th variable, and c_i^t and d_i^t are the

minimum and maximum of i th variable at t th iteration, which is defined as:

$$c_i^t = \text{Antlion}_j^t + c^t, \quad d_i^t = \text{Antlion}_j^t + d^t \tag{13}$$

where c^t indicates the vectors including the minimum of all variables at t th iteration, d^t indicates the vectors including the maximum of all variables at t th iteration, and Antlion_j^t shows the position of the selected j th ant lion at t th iteration.

3.3.3 Elitism Operation

Elitism is one of the most important characteristics of evolutionary algorithms. In the ALO algorithm, at any iteration the best ant lion obtained (solution of problem) is saved as an elite. Since the elite one is the fittest ant lion, it should be able to affect the movements of all the ants during iterations. In addition to this, the ants are not only designed to roam around the roulette wheel selected ant lion; rather, they are also allowed to move randomly around the elite ant lion simultaneously. For simplicity, the average of both random walks is considered to generate the new positions of the ant. The description of this operation is presented as (Mirjalili 2015):

$$\text{Ant}_i^t = \frac{(R_A^t + R_E^t)}{2} \tag{14}$$

where R_A^t and R_E^t are the random walks around the roulette wheel selected antlion, and the elite at t th iteration, and Ant_i^t indicates the position of i th ant at t th iteration.

3.3.4 Catching Preys/Re-building Traps

The final stage of the hunt is when an ant reaches the bottom of the pit and is caught in the ant lion’s jaw. After this stage, the ant lion pulls the ant inside the sand and consumes its body. For mimicking this process, it is assumed that catching prey occurs when ants become fitter (goes inside the sand) than its corresponding ant lion. An ant lion is then required to update its position to the latest position of the hunted ant to enhance its chance of catching new prey. The following equation represents this concept (Mirjalili 2015).

$$\text{Antlion}_j^t = \text{Ant}_i^t \quad \text{if } f(\text{Ant}_i^t) < f(\text{Antlion}_j^t) \tag{15}$$

where Ant_i^t indicates the position of i th ant at t th iteration and $f(\oplus)$ denotes the fitness function.

```

Static and dynamic input data
List of operating conditions
Power flow solver.
Small-disturbance stability solver.
Form the linear state-space equations for a given operating condition
Define the parameters:  $t_{max}$  (maximum number of iterations) and  $N_p$  (population size)
Randomly generate the initial population of ants and ant lions;
Compute the system eigenvalues in closed-loop
Calculate the fitness of  $i^{\text{th}}$  ants and ant lions ( $i = 1, 2, \dots, N_p$ );
Find the best ant lions and assume it as the elite (determined optimum);
while  $t < t_{max}$ ;
  for every ant;
    Select an ant lion using Roulette wheel;
    Update  $c$  and  $d$  using Eqs. (8) and (9);
    Create a random walk using Eqs. (12) and (13);
    Update the position of ant using Eq. (14);
  end for;
  Compute the system eigenvalues in closed-loop
  Calculate the fitness of all ants;
  Update ant lion according to Eq. (15);
  Update elite if an ant lion becomes fitter than the elite;
end while;
Return parameter PSS and POD;

```

Fig. 3 Pseudo-code of ant lion optimizer

3.4 Pseudo-code ALO Applied to Design PSS and POD

ALO-based algorithm begins with input data of the power system for all operating conditions. Positions of ant lions and ants are initialized randomly and saved in matrix M_{tal} , an element of this matrix contains one parameter of PSS or POD, and the i th row contains all parameters of PSSs and PODs to be optimized. Then the initial condition (power flow problem solution) of the system for all scenarios is calculated with software ANAREDE (2015) and saved. The system state-space matrix A is obtained and saved for all operating conditions. Eigenvalues are computed with PacDyn (2011) and saved. The operation of ALO may be summarized to the pseudo-code, as presented in Algorithm 1 (see Fig. 3). ALO is used for robust tuning of the parameters of PSSs and PODs. First row of M_{tal} will contain the best optimized parameters of PSSs and FACTS-PODs.

4 Simulations and Results

Two test systems are used for the application of the ant lion optimizer algorithm for robust design of PSSs and PODs. The first one is the New England–New York interconnected

system (Pal and Chaudhuri 2005), composed of 16 generators and 68 buses, which is used for tuning 12 PSS, 1 TCSC and 1 SVC. The second system is a Brazilian equivalent, modeled with 24 synchronous machines and 107 buses (Alves 2007), where the objective is to tune 16 PSS, 1 TCSC and 1 SVC in three loading scenarios, while maximizing the damping process. In the present paper, the eigenvalues were calculated by using the MATLAB© platform routines. All test systems used in the paper will be freely available by e-mail to anyone who requests them.

The time washout constant T_w of all stabilizers and PODs was defined as being 10 s. The time delay is considered to be 300 ms. Table 1 shows the bounds of controller parameters

Table 1 Parameter bounds

#	Parameters	68 bus		107 bus	
		Min.	Max.	Min.	Max.
PSS	Gain	0.1	50	0.1	30
	T_1-T_3	0.2	1.5	0.01	1.50
	T_2-T_4	0.02	0.15	0.01	1.50
POD	Gain	0.1	50	0.1	30
	T_1-T_3	0.05	1	0.01	1.50
	T_2-T_4	0.05	1	0.01	1.50

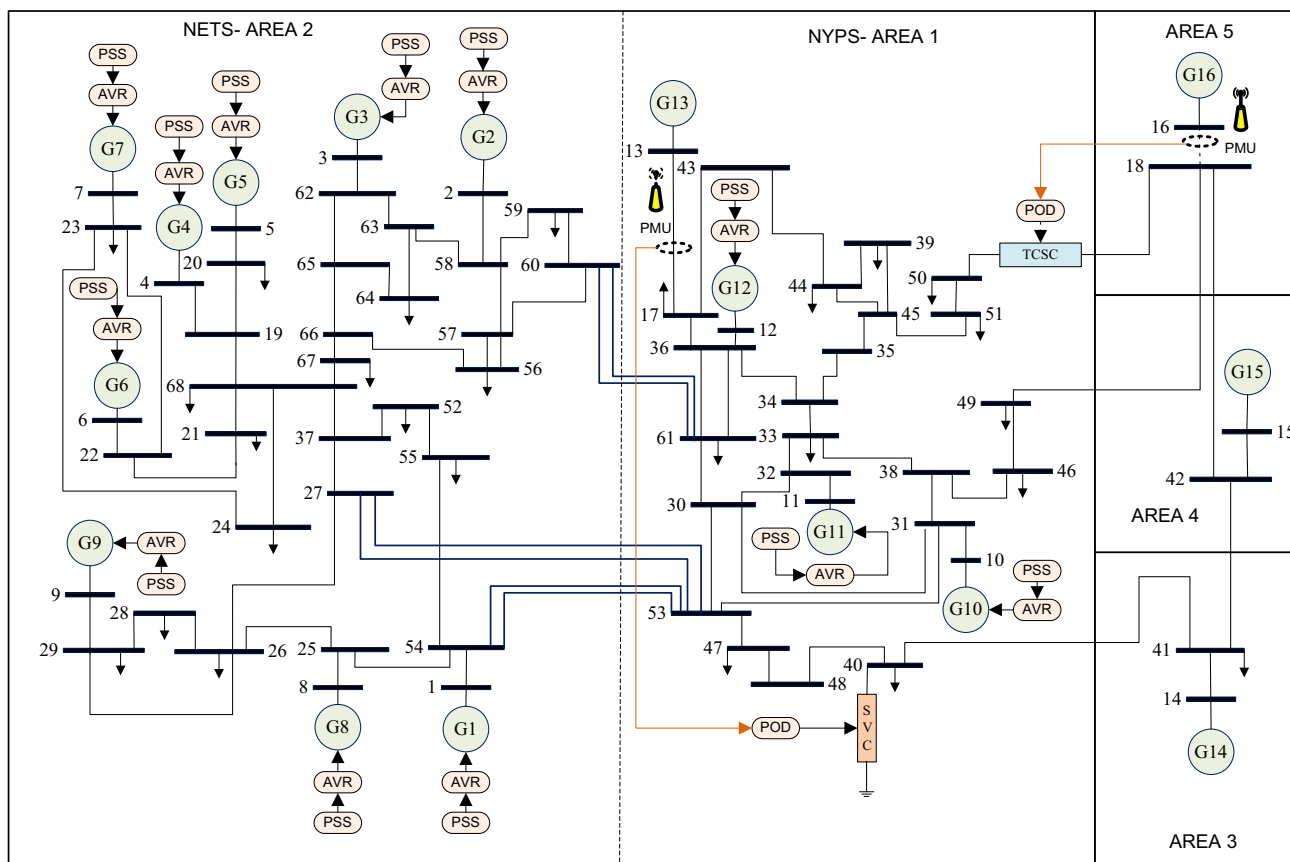


Fig. 4 Single-line diagram of NETS-NYPS system

used in both test systems. These bounds have been defined from typical values recommended in the literature about application of conventional PSSs to multimachine power systems.

The computer simulations were performed using a PC Intel (R) core (TM) i3, 3.30 GHz, with 8 GB of RAM.

4.1 68-Bus System (NETS-NYPS)

4.1.1 System Description

This is a 68-bus, 16-machine system, shown in Fig. 4. The detailed network parameters and the dynamic characteristics can be found in (Rogers 2000). The synchronous generators are represented by the fifth-order model, representing transient and subtransient effects in d and q axes, and do not consider the variation of the machine parameters and voltages with frequency. The stator dynamics are also neglected (PacDyn 2011). All generators are equipped with automatic voltage regulators-type IEEE standard DC exciter (DC4B), except generators 13–16, since they are equivalent areas. There are three transfer corridors between NETS and NYPS connecting buses 60–61, 53–54 and 27–53. Each of

Table 2 Operating conditions used for 68-bus system

Case	Operating condition	Type of load
1	Base case	100% CP
2	Base case	100% CC
3	Base case	50% CI and 50% CC
4	Outage tie-line 53–54	100% CP
5	Outage tie-line 61–60	100% CP
6	Outage tie-line 27–53	100% CP
7	Outage tie-lines 53–54/27–53	100% CP
8	Outage tie-lines 53–54/61–60	100% CP
9	Load + 10% of areas 3–5	100% CP
10	Load – 10% of areas 3–5	100% CP

the corridors has a double-circuit tie-line. Based on that information, ten operating conditions were considered, which are detailed in Table 2 (CI—constant impedance, CC—constant current and CP—constant power) (Jabr et al. 2010). Through

Table 3 Interarea oscillation modes for 68-bus system

Case #	Mode 1		Mode 2		Mode 3		Mode 4	
	ζ (%)	f (Hz)	ζ (%)	f (Hz)	ζ (%)	f (Hz)	ζ (%)	f (Hz)
1	3.32	0.8	-5.16	0.6	0.62	0.5	-1.02	0.4
2	3.37	0.8	-5.81	0.6	1.00	0.5	0.78	0.4
3	3.34	0.8	-5.59	0.6	0.74	0.5	-0.02	0.4
4	3.32	0.8	-3.88	0.6	-0.22	0.5	-2.84	0.4
5	3.32	0.8	-3.90	0.6	-0.61	0.5	-2.62	0.4
6	3.32	0.8	-5.00	0.6	0.53	0.5	-1.23	0.4
7	3.32	0.8	-3.40	0.6	-0.48	0.5	-3.29	0.4
8	3.32	0.8	-0.46	0.6	-2.59	0.5	-5.97	0.4
9	3.29	0.8	-5.41	0.6	1.13	0.5	-1.38	0.4
10	3.36	0.8	-4.90	0.6	0.13	0.5	-0.56	0.4

the modal analysis, it was verified that the system presents unstable local and interarea modes. Interarea modes area is shown in Table 3 and has a frequency within the range of 0.8–0.4 Hz.

4.1.2 Installation Location of the FACTS and Feedback Signal Selection of the POD

In order to enhance the interconnected ability, one SVC is installed on bus 40, and one TCSC is installed between bus 50 and bus 18. PSSs installed on generators 1–12 should dampen local modes. In contrast, the TCSC and SVC controllers should dampen the interarea modes, these FACTS being equipped with POD. The SVC-POD should be designed to dampen interarea 4 and 2 modes, as these modes are more correlated with areas 1 and 2. Furthermore, the POD of the TCSC should dampen modes 3 and 1, as they are more correlated with areas 3, 4 and 5 (Deng et al. 2015). From the residue values, feedback signals for SVC and TCSC damping controllers have active power flow on Line 13–17 and Line 16–18—in other words, P_{13-17} e P_{16-18} , respectively. These signals are remote, so there is a time delay. The state-space representation of the closed-loop system has 215 state variables.

4.1.3 Tuning of Controllers

For the tuning of the PSSs and PODs it was specified in the design that all modes of oscillation must have a damping coefficient above 10%. The parameters obtained through the proposed methodology considering the ten cases of contingencies are presented in Table 4. The coordinated design of the PSS and POD applying the ALO algorithm proved to be effective in shifting all modes of oscillation into the desired

Table 4 Optimized parameters of PSSs and PODs for 68-bus system

#	Gain	T_1	T_2	T_3	T_4
<i>PSS</i>					
1	8.86	0.3663	0.0235	0.3924	0.0445
2	8.25	0.4924	0.0242	0.3204	0.0540
3	2.28	0.8473	0.0464	0.2048	0.0247
4	3.40	0.7281	0.0223	0.2105	0.0318
5	1.80	0.3204	0.0229	0.5683	0.0202
6	2.05	0.8498	0.1228	0.2735	0.0312
7	10.75	1.0615	0.0392	0.5654	0.0390
8	2.69	0.3899	0.0285	0.2380	0.0453
9	26.44	0.5512	0.0264	0.3061	0.0294
10	28.37	0.2058	0.0247	0.3722	0.0513
11	6.25	0.2543	0.0597	0.2058	0.0926
12	38.73	0.9073	0.0211	0.2618	0.0459
<i>TCSC-POD</i>					
50–18	22.70	0.0888	0.8098	0.2337	0.2521
<i>SVC-POD</i>					
40	2.90	0.0521	0.5442	0.4806	0.3111

region, according to Fig. 5b, which presents a comparison between the open-loop and closed-loop pole locations.

4.2 Brazilian Equivalent System

4.2.1 System Description

The 107-bus test system has 24 bus generation and 230 circuits. Details of the data are given in (Alves 2007), and a simplified single-line diagram is shown in Fig. 6. Each of the machines is assumed to be equipped with a static excitation system having a time constant $T_a = 0,05s$ and a moderate gain given by $T'_{d0}/2T_a$, where T'_{d0} is the generator d -axis

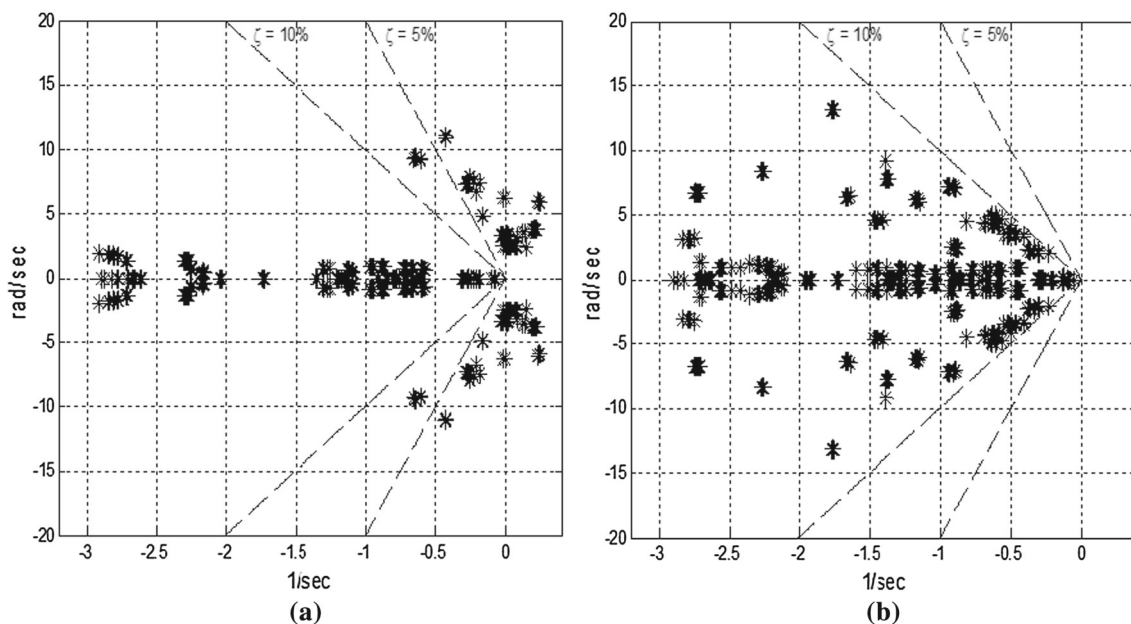
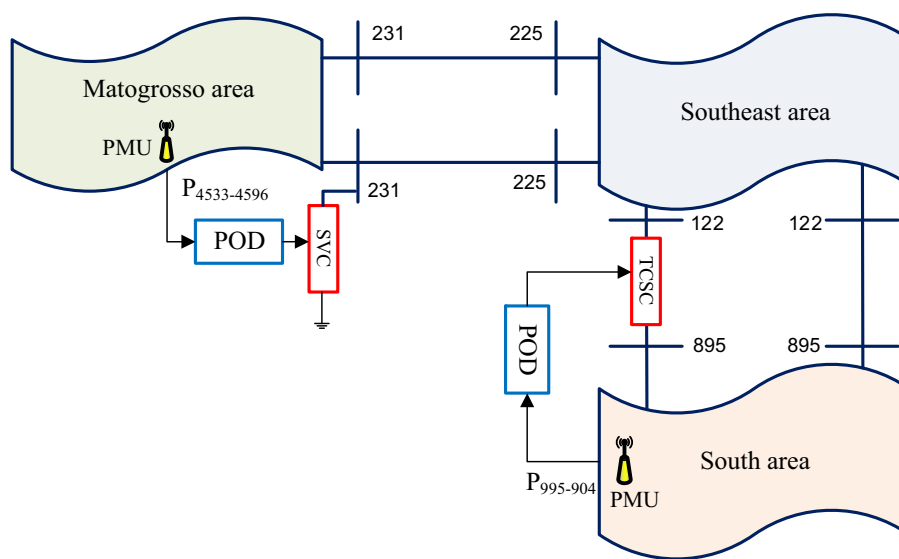


Fig. 5 Open-loop poles map (a) and closed-loop poles map (b) considering the ten operating conditions of NETS-NYPS system

Fig. 6 Single-line diagram of Brazilian 107-bus system



open-circuit transient constant (Jabr et al. 2010). Besides AVR, the speed governors are represented in detail.

For this system, heavy (base case—scenario 1), average (load—15% of base case—scenario 2) and light (load—25% of base case—scenario 3) loading conditions were considered during the tuning process. Figure 7a shows the mapping of the open-loop poles for three operating conditions. For these conditions, there are two interarea modes and several local modes. The frequencies and damping ratio of the interarea modes are exposed in Table 5.

4.2.2 Installation Location of the FACTS and Feedback Signal Selection of the POD

The local modes will be damped by the PSS, while the interarea modes by the FACTS. Based on participation factors, 16 PSSs were installed in the system under study. Based on the analysis of the shape modes, it was observed that interarea mode 1 involves the machines of the Mato Grosso and Southeast Area against the South Area. In contrast, interarea mode 2 involves the machines of the Mato Grosso Area against the machines of the Southeast Area. In this way, two FACTS con-

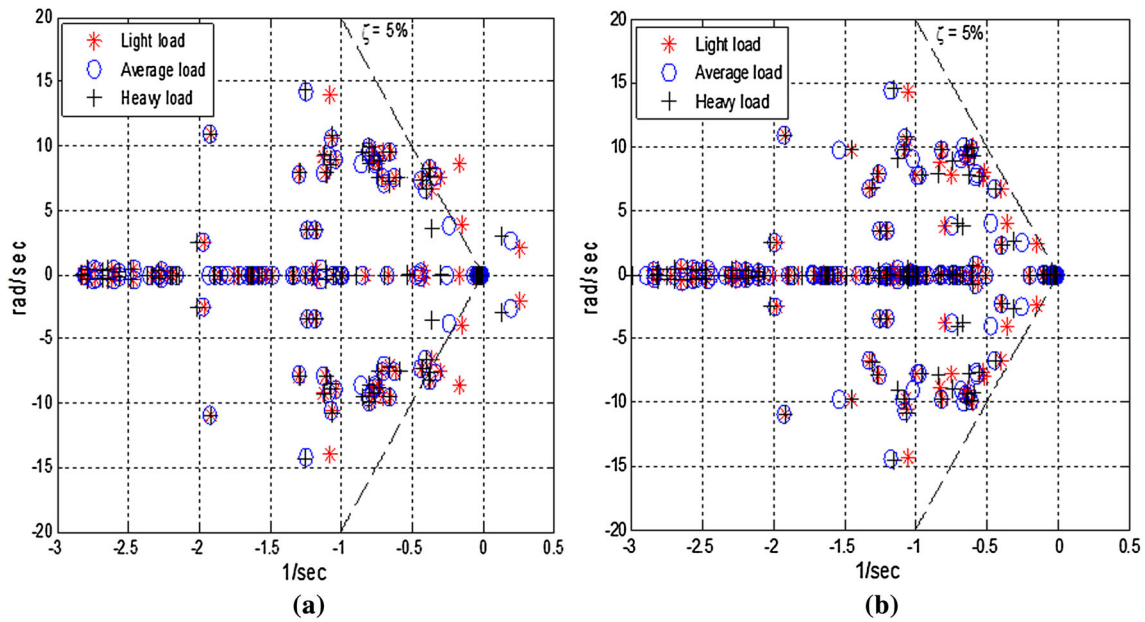


Fig. 7 Open-loop poles map (a) and closed-loop poles map (b) considering the three operating conditions of Brazilian 107-bus system

Table 5 Interarea oscillation modes for 107-bus system

Case	Mode 1: Mato Grosso/Southeast versus South		Mode 2: Mato Grosso versus Southeast		Power flow (MW)	
	ζ (%)	f (Hz)	ζ (%)	f (Hz)	Line 122–895	Line 231–225
Light load	– 12.40	0.33	3.75	0.61	1839.5	119.8
Average load	– 7.59	0.41	6.07	0.61	1415.3	187.9
Heavy load	– 4.42	0.46	10.0	0.56	607.1	319.4

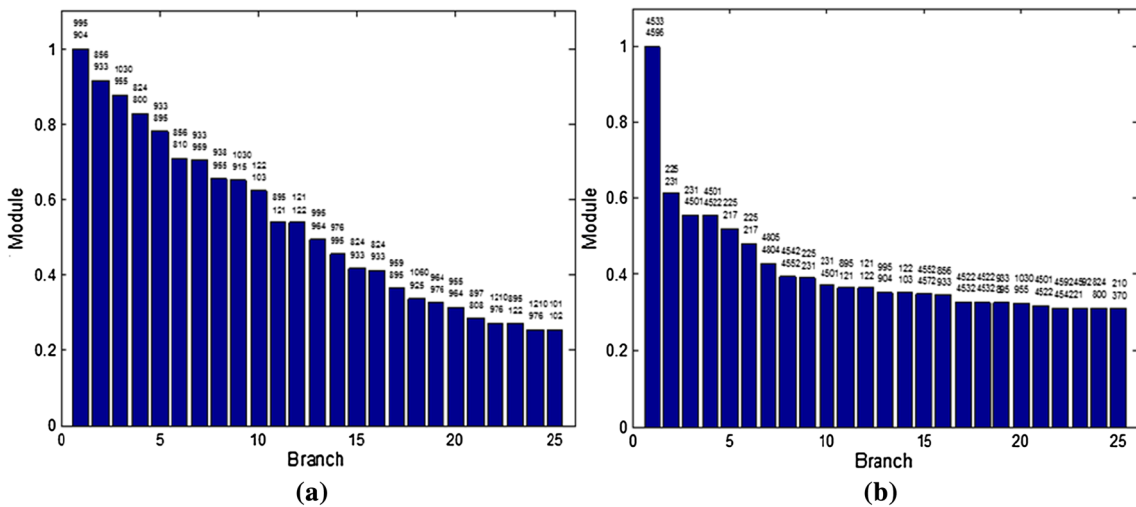


Fig. 8 Modal residues of Brazilian 107-bus system: mode 1 (a) and mode 2 (b)

trollers were installed in the system. A TCSC was installed in the line between buses #122 and #895 that interconnect the Southeast and South Areas in order to damp interarea mode 1,

and a SVC was in bus 231 in order to damp interarea mode 2. The input signals of the corresponding PODs were obtained from the residue analysis, which are shown in Fig. 8. For

Table 6 Data of nonlinear simulations

System	Simulation
68 Bus	1 A three-phase fault at bus 53 is simulated for 70 ms in one of the tie-lines between bus 53 and bus 54. The fault is cleared by the removal of the faulted circuit
	2 A 5% step increase in the voltage reference of the excitation system of machine 12
107 Bus	1 A three-phase fault at bus 138 is simulated for 50 ms in one of the lines between bus 138 and bus 140. The fault is cleared by the removal of the faulted circuit
	2 A three-phase fault at bus 126 is simulated for 120 ms in one of the lines between bus 126 and bus 120. The fault is cleared by the removal of the faulted circuit

mode 1, which will be damped by the POD corresponding to the TCSC, the input signal will be the active power flow on Line 995–904. In the case of interarea mode 2, whose damping will be provided by the POD of the SVC, the input signal will be the active power flow on Line 4533–4596.

4.2.3 Tuning of Controllers

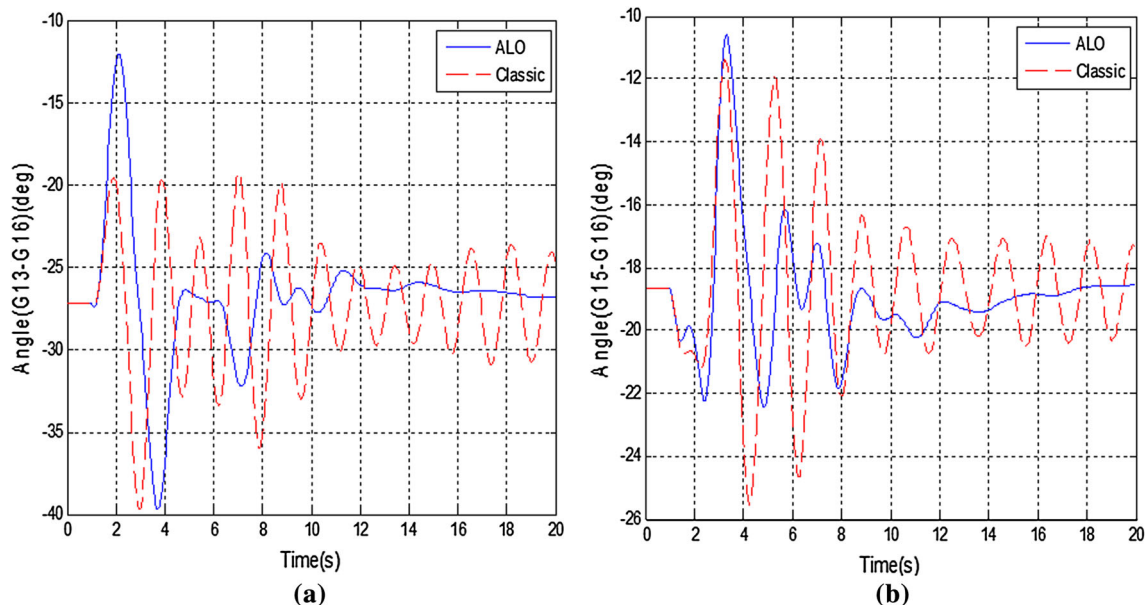
The state-space representation of the closed-loop system has 326 state variables. For the tuning of the PSSs and PODs it was specified in design that all modes of oscillation must have a damping coefficient above 5%. Figure 7b shows the closed-loop eigenvalues after tuning 16 PSSs and 2 PODs. Note that

the system becomes stable with a minimum damping ratio greater than 5% for all three operating points.

4.3 Transient Stability Analysis

In practice, any stabilizer design needs to be checked for robustness under different operating conditions using a transient stability simulation (Jabr et al. 2010). Time-domain simulations use the ANATEM software (2010). Limit inputs of AVR and PSS were defined by the intervals $[-10, 10]$ and $[-0.1, 0.15]$, respectively. Two cases were considered for each test system and are presented in Table 6.

Figures 9 and 10 illustrate the behavior of the rotor angle of generators 13 (Fig. 9a) and 15 (Fig. 9b) with respect to the generator 16 and the speed deviation of generators 12 (Fig. 10a) and 3 (Fig. 10b), respectively, for the simulations performed in the 68-bus system. The legend “Classic” used in Figs. 9 and 10 means that the PSSs parameters used in these simulations were extracted from (Rogers 2000). In both cases, the power system, with the inclusion of PSSs and FACTS-PODs tuned by the ALO algorithm, stabilizes around 12 s. In addition, Figs. 11 and 12 show the active power flow behavior between one of the tie-lines 231–225 and the rotor angles of all machines relative to the machine 18, respectively. In Fig. 11, increasing oscillations of the active power flow are observed before inclusion of PSSs and FACTS-PODs. With the installation and tuning of these controllers, the oscillations were damped and the damping coefficients are higher than the minimum required. Note in Fig. 12a that the amplitudes of the rotor angles grow over time, so the system is unstable without installation of PSSs and FACTS-

**Fig. 9** System responses with case 1: 68-bus system

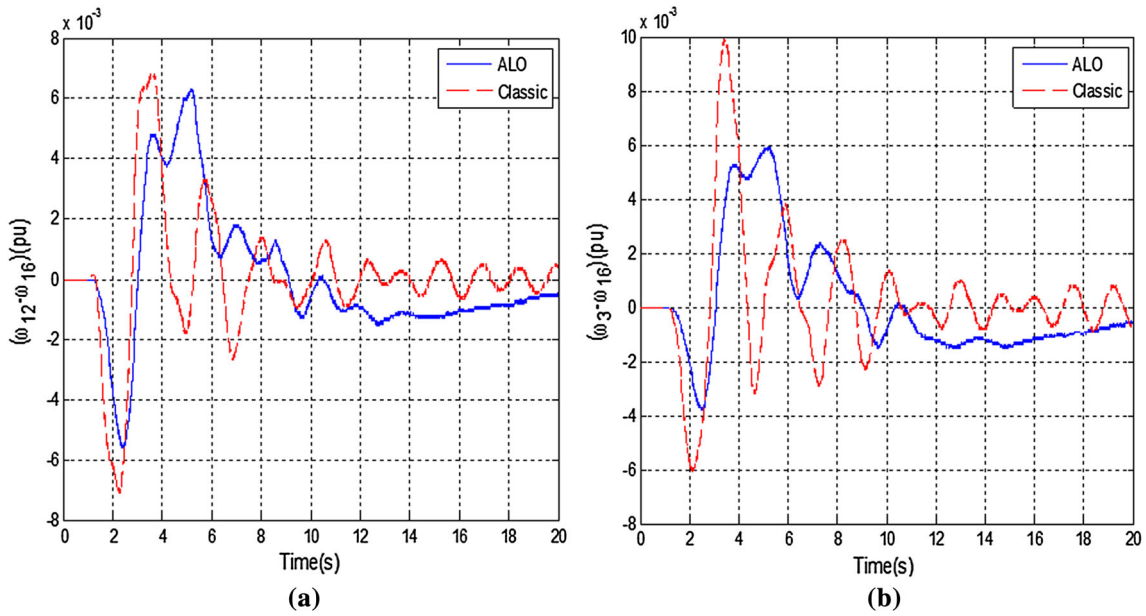


Fig. 10 System responses with case 2: 68-bus system

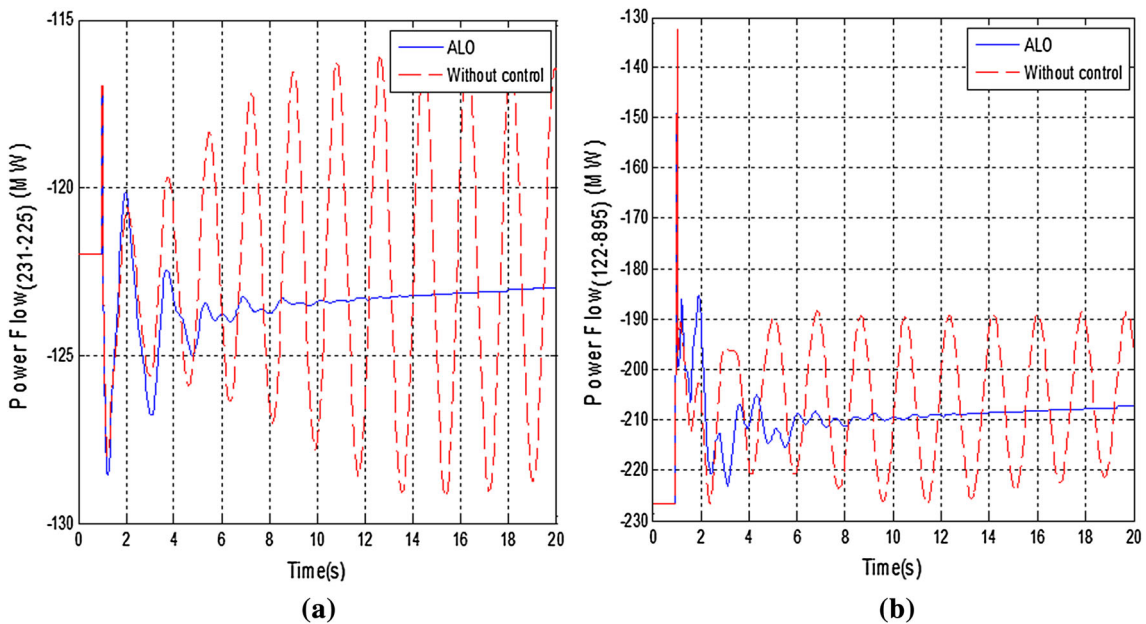


Fig. 11 System responses with case 1: 107-bus system

PODs. However, it can be seen clearly in Fig. 12b the rapid damping of the oscillations of the rotor angles and the recovery of the stability of the system due to insertion of PSSs and FACTS-PODs. The results demonstrate that the parameters obtained through the ALO technique are robust for nonlinear simulations of transient stability.

Two performance indices that reflect the settling time (PL_1) and overshoots (PL_2) as a function of the machine speed deviation are defined in Eqs. (16) and (17), where N_{ger} is the number of machines, and t_{sim} is the simulation time

(Abido and Abdel-Magid 2002). Results are presented in Table 7, where the symbol * indicates that for the 68-bus system, the parameters used for the PSSs are in accordance with reference (Rogers 2000). In contrast, for the 107-bus system, it is equivalent to the system without PSS and FACTS-POD.

$$PL_1 = \sum_{k=1}^{N_{ger}} \int_{t=0}^{t=t_{sim}} [t \Delta \omega_k(t)]^2 dt \tag{16}$$

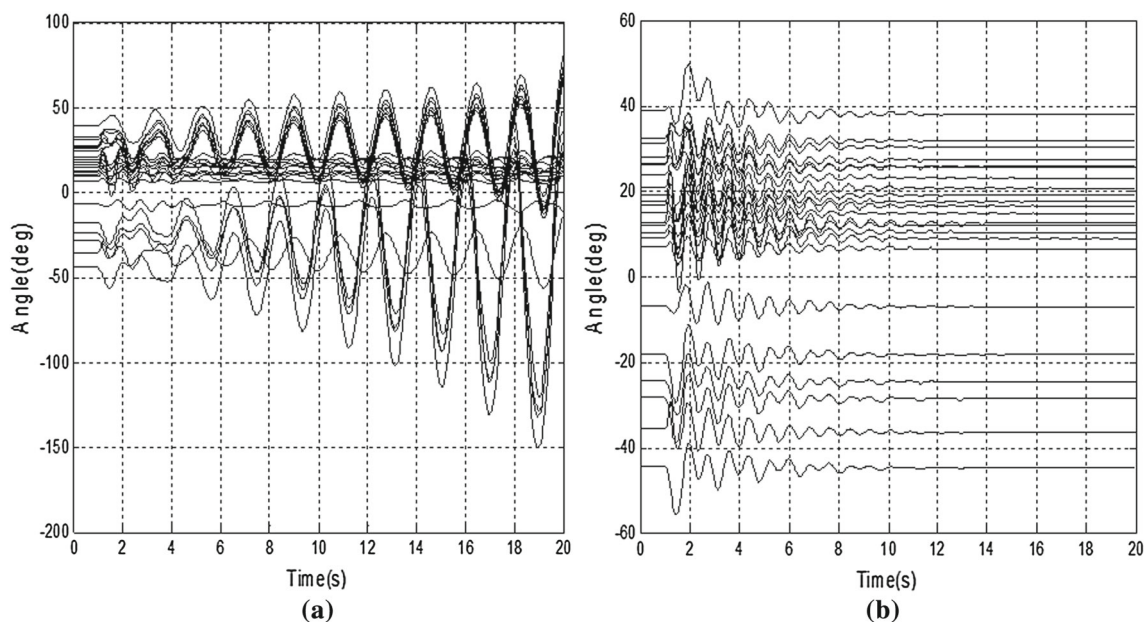


Fig. 12 System responses with case 2: 107-bus system

Table 7 Performance indices

Indices	System	68 bus		107 bus	
		1	2	1	2
PL ₁	ALO	2.1E−3	2.01E−1	2.9E−2	4.7E−3
	*	10.9E−3	3.01E−1	5.2E−2	6.4E−1
PL ₂	ALO	1.31E−4	1.02E−3	1.8E−4	1.3E−4
	*	1.37E−4	1.36E−3	7.4E−4	2.9E−3

$$PL_2 = \sum_{k=1}^{N_{ger}} \int_{t=0}^{t=t_{sim}} [\Delta\omega_k(t)]^2 dt \tag{17}$$

4.4 Comparison with Other Techniques

Exploration (global search) and exploitation (local search) are characteristics of the ant lion optimizer to efficiently approximate the global optimum of constrained optimization problems such as robust tuning of PSSs and PODs.

Application results of ALO to test systems 68 bus and 107 bus demonstrate that robust tuning of PSSs and FACTS-PODs led to obtain damping values that may be competitive or even higher than other ones calculated with conventional optimization methods and AI-based techniques. A routine for constrained nonlinear optimization based on sequential quadratic programming, available in the MATLAB and algorithm PSO, was used for comparison with the algorithm ALO. Three cases were simulated, changing only the initial values of the decision variables. The results are shown in Table 8, where the symbol* means $\zeta_{min} < 0$. Table 8 indicates that the SQP technique is very dependent on the

Table 8 Minimum damping ratio (%)

System	x_0	ALO	PSO	SQP
68 Bus	Rand	11.78	9.78	*
	lb	11.08	0.36	9.18
	ub	9.68	*	*
107 Bus	Rand	5.96	5.65	6.72
	lb	6.19	4.25	8.05
	ub	7.27	5.91	7.76

initial estimate of solution. In contrast, ALO presented the best values, on average, for the two test systems.

5 Conclusions

In this work, a methodology based on the ant lion optimizer for robust tuning of PSSs and FACTS-PODs of interconnected multimachine power systems has been proposed.

The model of the robust tuning process corresponds to a nonlinear optimization problem with an objective function

for maximizing the minimum damping of the closed-loop system under multiple operating conditions.

The application results of ALO-based methodology demonstrated an efficient damping of local and interarea oscillations of two interconnected test systems. For the NETS-NYPS test system, the best minimum damping calculated with ALO is greater than most results reported in respective literature. For the 107-bus test system, results of robust tuning of PSSs and FACTS-PODs using ALO ensured damping ratios greater than typical values obtained with other conventional and AI-based methods.

Nonlinear time-domain simulations validated the robust tuning of PSSs and FACTS-PODs using ALO, and all results have shown that the optimized parameters of those controllers guaranteed the stability of the test systems.

Thus, the ALO-based methodology has demonstrated to be an efficient alternative to solve the robust tuning of PSSs and FACTS-PODs of multimachine power systems.

Acknowledgements The authors would like to thank the “Coordination for the Improvement of Higher Education Personnel” (CAPES) for supporting this work and CEPEL for granting the license to use the programs PacDyn and ANATEM.

References

- Abid, M. A., & Abdel-Magid, Y. L. (2002). Optimal design of power system stabilizers using evolutionary programming. *IEEE Transactions on Energy Conversion*, 17(2), 429–436.
- Afzalan, E., & Joorabian, M. (2013). Analysis of the simultaneous coordinated design of STATCOM-based damping stabilizers and PSS in a multimachine power system using the seeker optimization algorithm. *International Journal of Electrical Power & Energy Systems*, 53, 1003–1017.
- Ali, E. S., & Abd-Elazim, S. M. (2012). Coordinated design of PSSs and TCSC via bacterial swarm optimization algorithm in a multimachine power system. *International Journal of Electrical Power & Energy Systems*, 36(1), 84–92.
- Alves, W. F. (2007). Proposition of test-systems to power systems analysis (in Portuguese). MSc Dissertation, Fluminense Federal University, Brazil.
- ANAREDE-Power System Network Analysis V. 10.0.2. (2015). Electrical Energy Research Center (CEPEL). Rio de Janeiro, Brazil, User’s manual.
- ANATEM- Analysis of Electromechanical Transients V. 10.04.05. (2010). Electrical Energy Research Center (CEPEL). Rio de Janeiro, Brazil, User’s manual.
- Cai, L., & Erlich, I. (2005). Simultaneous coordinated tuning of PSS and FACTS damping controllers in large power systems. *IEEE Transactions on Power Systems*, 20(1), 294–300.
- Chaudhuri, B., Majumder, R., & Pal, B. C. (2004). Wide-area measurement-based stabilizing control of power system considering signal transmission delay. *IEEE Transactions on Power Systems*, 19(4), 1971–1979.
- Chaudhuri, B., & Pal, B. C. (2004). Robust damping of multiple swing modes employing global stabilizing signals with a TCSC. *IEEE Transactions on Power Systems*, 19(1), 499–506.
- Chen, Z., Yuan, X., Yuan, Y., Iu, H. H. C., & Fernando, T. (2017). Parameter identification of integrated model of hydraulic turbine regulating system with uncertainties using three different approaches. *IEEE Transactions on Power Systems*, 32(5), 3482–3491.
- Deng, J., Li, C., & Zhang, X. (2015). Coordinated design of multi-robust FACTS damping controllers: a BMI-based sequential approach with multi-model systems. *IEEE Transactions on Power Systems*, 30(6), 3150–3159.
- Fertin, A., & Casas, J. (2007). Orientation towards prey in antlions: efficient use of wave propagation in sand. *Journal of Experimental Biology*, 210(19), 3337–3343.
- Fortes, E. V., Araujo, P. B., & Macedo, L. H. (2016). Coordinated tuning of the parameters of PI, PSS and POD controllers using a specialized Chu–Beasley’s genetic algorithm. *Electric Power Systems Research*, 140, 708–721.
- Fortes, E. V., Macedo, L. H., Araujo, P. B., & Romero, R. (2018). A VNS algorithm for the design of supplementary damping controllers for small-signal stability analysis. *International Journal of Electrical Power & Energy Systems*, 94, 41–56.
- Gamino, B. R., & Araujo, P. B. (2017). Application of a basic variable neighborhood search algorithm in the coordinated tuning of PSS and POD controllers. *Journal of Control, Automation and Electrical Systems*, 28(4), 470–481.
- Guillette, L. M., Hollis, K. L., & Markarian, A. (2009). Learning in a sedentary insect predator: antlions (Neuroptera: Myrmeleontidae) anticipate a long wait. *Behavioural Processes*, 80(3), 224–232.
- Hassan, L. H., Moghavvemi, M., Almurib, H. A. F., & Muttaqi, K. M. (2014). A coordinated design of PSS and UPFC-based stabilizer using genetic algorithm. *IEEE Transactions on Industry Applications*, 50(5), 2957–2966.
- Jabr, R. A., Pal, B. C., & Martins, N. (2010). A sequential conic programming approach for the coordinated and robust design of power system stabilizers. *IEEE Transactions on Power Systems*, 25(3), 1627–1637.
- Kamwa, I., Grondin, R., & Trudel, G. (2005). IEEE PSS2B versus PSS4B: the limits of performance of modern power system stabilizers. *IEEE Transactions on Power Systems*, 20(2), 903–915.
- Ke, D. P., Chung, C. Y., & Xue, Y. (2011). An eigenstructure-based performance index and its application to control design for damping inter-area oscillations in power system. *IEEE Transactions on Power Systems*, 26(4), 2371–2380.
- Khaleghi, M., Farsangi, M. M., Nezamabadi-pour, H., & Lee, K. Y. (2011). Pareto-optimal design of damping controllers using modified artificial immune algorithm. *IEEE Transactions on System, Man, and Cybernetics, Part C (Applications and Reviews)*, 41(2), 240–250.
- Kundur, P. (1994). *Power system stability and control*. New York: McGraw-Hill.
- Lei, X., & Povh, D. (2001). Optimization and coordination of damping controls for improving system dynamic performance. *IEEE Transactions on Power Systems*, 16(3), 473–480.
- Martins, L. F. B., Araujo, P. B., Forte, E. V., & Macedo, L. H. (2017). Design of the PI-UPFC-POD and PSS damping controllers using an artificial bee colony algorithm. *Journal of Control, Automation and Electrical Systems*, 28(6), 762–773.
- Menezes, M. M., Araujo, P. B., & Valle, D. B. (2016). Design of PSS and TCSC damping controller using particle swarm optimization. *Journal of Control, Automation and Electrical Systems*, 27(5), 554–561.
- Milano, F. (2016). Small-signal stability analysis of large power systems with inclusion of multiple delays. *IEEE Transactions on Power Systems*, 31(4), 3257–3266.
- Mirjalili, S. (2015). The ant lion optimizer. *Advances in Engineering Software*, 83, 80–98.
- PacDyn- Small Stability Analysis and Control V. 9.3.4. (2011). CEPEL, Centro de Pesquisas de Energia Elétrica. Rio de Janeiro, User’s manual.

- Pal, B., & Chaudhuri, B. (2005). *Robust control in power systems*. New York: Springer.
- Pourbeik, P., & Gibbard, M. J. (1998). Simultaneous coordination of power system stabilizers and FACTS devices stabilizers in a multi-machine power system for enhancing dynamic performance. *IEEE Transactions on Power Systems*, 13(2), 473–479.
- Rogers, G. (2000). *Power system oscillations*. New York: Springer.
- Shakarami, M. R., & Davoudkhani, I. F. (2016). Wide-area power system stabilizer design based on grey wolf optimization algorithm considering the time delay. *Electric Power Systems Research*, 133, 149–159.
- Shayeghi, H., Safari, A., & Shayanfar, H. A. (2010). PSS and TCSC damping controller coordinated design using PSO in a multi-machine power system. *Energy Conversion and Management*, 51(12), 2930–2937.
- Simfukwe, D. D., Pal, B. C., Jabr, R. A., & Martins, N. (2012). Robust and low-order design of flexible AC transmission system and power system stabilizers for oscillation damping. *IET Generation, Transmission and Distribution*, 6(5), 445–452.
- Simões, A. M., Savelli, D. C., Pellanda, P. C., Martins, N., & Apkarian, P. (2009). Robust design of a TCSC oscillation damping controller in a weak 500-kV interconnection considering multiples power flow scenarios and external disturbances. *IEEE Transactions on Power Systems*, 24(1), 226–236.
- Stillinger, F. H., & Weber, T. A. (1988). Nonlinear optimization simplified by hypersurface deformation. *Journal of Statistical Physics*, 52(5–6), 1429–1445.
- Werner, H., Korba, P., & Yang, T. C. (2003). Robust tuning of power system stabilizers using LMI-techniques. *IEEE Transactions on Control Systems Technology*, 11(1), 147–152.
- Yang, N., Liu, Q., & McCalley, J. D. (1998). TCSC controller design for damping interarea oscillations. *IEEE Transactions on Power Systems*, 13(4), 1304–1310.
- Yao, W., Jiang, L., Wu, Q. H., Wen, J. Y., & Cheng, S. J. (2011). Delay-dependent stability analysis of the power system with a wide-area damping controller embedded. *IEEE Transactions on Power Systems*, 26(1), 233–240.